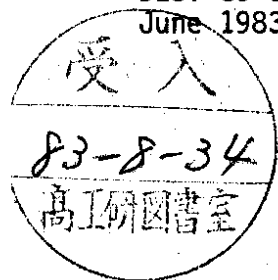


DEUTSCHES ELEKTRONEN-SYNCHROTRON **DESY**

DESY 83-054

June 1983



MEASUREMENT OF TRANSVERSE MOMENTA IN e^+e^- ANNIHILATION JETS AT PETRA

by

PLUTO Collaboration

ISSN 0418-9833

NOTKESTRASSE 85 · 2 HAMBURG 52

DESY behält sich alle Rechte für den Fall der Schutzrechtserteilung und für die wirtschaftliche Verwertung der in diesem Bericht enthaltenen Informationen vor.

DESY reserves all rights for commercial use of information included in this report, especially in case of filing application for or grant of patents.

**To be sure that your preprints are promptly included in the
HIGH ENERGY PHYSICS INDEX ,
send them to the following address (if possible by air mail) :**

**DESY
Bibliothek
Notkestrasse 85
2 Hamburg 52
Germany**

MEASUREMENT OF TRANSVERSE MOMENTA IN e^+e^- ANNIHILATION JETS AT PETRA

PLUTO COLLABORATION

Ch. Berger, H. Genzel, W. Lackas, J. Pielorz, F. Raupach, W. Wagner
I. Phys. Institut der RWTH Aachen¹, Germany

L.H. Fløio, A. Klovnig, E. Lillestøl, J.M. Olsen
University of Bergen², Norway

J. Bürger, L. Criegee, Ch. Dehne, A. Deuter, A. Eskreys³, G. Franke, M. Gaspero⁴,
Ch. Gerke⁵, U. Jacobs, G. Knies, B. Lewendel, U. Maurus, J. Meyer, U. Michelsen,
K.H. Pape, B. Stella⁴, U. Timm, G.G. Winter, S.T. Xue⁶, M. Zachara⁷,
P. Maloschek, W. Zimmermann

Deutsches Elektronen-Synchrotron DESY, Hamburg, Germany

P.J. Bussey, S.L. Cartwright, J.B. Dainton, B.T. King, C. Raine, J.M. Scarr
I.O. Skillicorn, K.M. Smith, J.C. Thomson
University of Glasgow, U.K.⁸

O. Achtenberg, L. Boesten, D. Burkart, K. Diehlmann, V. Hepp⁹, H. Kapitza,
B. Koppitz, M. Krüger, W. Lührsen¹⁰, M. Poppe, H. Spitzer, R. van Staa
II. Institut für Experimentalphysik der Universität Hamburg¹, Germany

C.Y. Chang, R.G. Glasser, R.G. Kellogg, S.J. Maxfield, R.O. Polvado, B. Sechi - Zorn,
J.A. Skard, A. Skuja, A.J. Tytka, G.E. Welch, G.T. Zorn
University of Maryland¹¹, U.S.A.

F. Almeida, A. Bäcker, F. Barreiro, S. Brandt, K. Derikum, C. Grupen, H.J. Meyer⁵,
H. Müller, B. Neumann, M. Rost, K. Stupperich, G. Zech
Universität-Gesamthochschule Siegen¹, Germany

G. Alexander, G. Bella, Y. Ggat, J. Grunhaus
Tel-Aviv University¹², Israel

H.J. Daum, H. Junge, K. Kraski, C. Maxeiner, H. Maxeiner, H. Meyer, D. Schmidt
Universität - Gesamthochschule Wuppertal¹, Germany

Hamburg, June 1983

- 1) Supported by the BMFT, Germany
- 2) Partially supported by the Norwegian Council for Science and Humanities
- 3) Now at Institute of Nuclear Physics, Cracow
- 4) Rome University, partially supported by I.N.F.N., Sezione di Rome, Italy
- 5) Now at CERN
- 6) Now at Institute of High Energy Physics, Academia Sinica, Peking, The People's Republic of China
- 7) On leave from Institute of Nuclear Physics, Cracow
- 8) Supported by the UK Science and Engineering Research Council
- 9) Now at Heidelberg University, Germany
- 10) Now at LBL
- 11) Partially supported by Department of Energy, USA
- 12) Partially supported by the Israeli Academy of Sciences and Humanities - Basic Research Foundation

ABSTRACT

Transverse particle momenta have been measured in e^+e^- annihilation into hadrons at c.m. energies between 9.4 and 31.6 GeV. The data are fully corrected for detector effects and radiation in the initial state. A comparison is made with recent QCD calculations.

The fragmentation of fast moving quarks produces hadrons with limited transverse momenta. This leads to the formation of jets which become more collimated with increasing quark energy, in accordance with many observations in the 4 - 10 GeV range. On the other hand, QCD relates the jet width to gluon emission, and predicts growing transverse momenta, also called jet broadening, at higher energies [1]. These effects have been observed in jets produced in both e^+e^- annihilation and deep inelastic lepton-hadron scattering [2,3].

The presently available data extend from low energies, where fragmentation dominates, into a transition region where QCD features clearly emerge in some observables, but still have to be disentangled from strong and not well understood fragmentation effects.

Since the interplay between perturbative QCD and fragmentation effects appears to be different in different observables, a quantitative investigation of QCD requires the study of a variety of jet measures.

The aim of this paper is a presentation of several quantities related to the transverse spread of jets, $\langle P_T \rangle$, $\langle P_T^2 \rangle$, $\langle \sum P_T \rangle$ and $\langle \sum P_T^2 \rangle$. The data presented are corrected for detector effects and for initial state radiation (which also produces detector-dependent biases), so that they can be directly compared with theoretical predictions as well as with corrected data from reactions other than e^+e^- annihilation. As an example a comparison to some recent predictions of perturbative QCD in the leading log approximation will be presented.

The data which have been used in the present analysis have been obtained with the PLUTO detector at the storage rings DORIS and PETRA at DESY, Hamburg. Details on the experimental set-up have been published elsewhere [4]. For a rough orientation we summarize the main features of the detector as follows: a) PLUTO is a magnetic detector with a field of 1.64 Tesla provided by a superconducting solenoid, b) Charged particles are tracked in an inner detector consisting of thirteen layers of cylindrical proportional chambers covering 87% of 4π , c) Neutrals are detected with the help of barrel and end-cap lead scintillator shower counters covering together 96% of 4π .

The data selection criteria demand that a) the visible energy should be greater than half the nominal c.m. energy, b) at least four charged tracks should have a common interaction vertex centered within ± 4 cm around the bunch-bunch collision point, and c) the angle ϑ between the jet axis and the e^+ beam direction should satisfy $|\cos \vartheta| < 0.75$. Final states selected this way were visually inspected and found to contain a negligible

contamination from showering cosmic ray particles, QED events and from beam-gas interactions (<2% total).

The data used in the present analysis have been obtained at c.m. energies of 7.7, 9.4, 12, 13, 17, 22, 27.6 GeV and in an energy scan between 30 and 31.6 GeV. The analysis for a given event proceeds as follows:

- a. The thrust axis [5] is determined from charged and neutral particles
- b. The transverse momentum P_T of the final state particles with respect to this axis is measured and used to determine the mean values $\langle P_T \rangle$ and $\langle P_T^2 \rangle$ as well as the mean total transverse momenta $\langle \sum P_T \rangle$ and $\langle \sum P_T^2 \rangle$ with the sum running over all particles including neutrals.

In order to correct the mean values for detector acceptance and resolution as well as for radiation in the initial state the above analysis procedure has been applied to two samples of Monte Carlo generated events, one with an ideal final state undisturbed by detector effects and by initial state radiation, and the other after including a complete simulation of the apparatus, the selection criteria and radiative effects in the initial state. From a comparison of the observables obtained from these two samples a correction factor was derived and applied to the data. At low energies the Field-Feynman model was used as a Monte Carlo generator [6] while at energies above 17 GeV QCD corrections were taken into account according to Hoyer et al. [7], including c- and b-quarks. These two sets of Monte Carlo generators have been found to adequately describe our data [2].

The corrections obtained were found to be reasonably small, ranging from 3% at 7.7 GeV to 20% at 30 GeV for $\langle P_T \rangle$, and smaller than 5% at all energies for $\langle \sum P_T \rangle$. As a check the whole analysis was repeated using only charged particles. The correction factors were found correspondingly larger for the case of jet quantities like $\langle \sum P_T \rangle$ but smaller, $\approx 10\%$ at 30 GeV, for single particle averages like $\langle P_T \rangle$. In all cases however the corrected values for the sample of charged particles only were compatible with those previously obtained for the charged and neutral sample.

Finally we have investigated what biases might be introduced by the jet axis finding algorithm. To this end we repeated the whole analysis using three different approaches:

a. Rather than defining one axis as given by thrust we partitioned every event into two hemispheres by defining two independent axes along which the sum of the longitudinal momenta of final state hadrons was maximized. The algorithm described in ref. [12] was used. The corrected values obtained using this procedure agreed within errors with those from the thrust algorithm. This means that radiative effects which lead to non-collinear jets are adequately corrected for.

b. We defined the jet axis as the sphericity axis [8]. The resulting values for $\langle P_T \rangle$ and $\langle P_T^2 \rangle$ measured with respect to the sphericity axis are, as expected, systematically somewhat lower than those obtained with respect to thrust. The differences are in most cases statistically significant.

c. In the Monte Carlo sample representing final states undisturbed by detector effects we introduced the jet axis as that of the most energetic parton. The values for $\langle P_T \rangle$ and $\langle P_T^2 \rangle$ thus corrected at the quark axis level were within error bars compatible with those obtained with respect to the thrust axis, though systematically slightly larger.

The final results for $\langle P_T \rangle$, $\langle P_T^2 \rangle$, $\langle \sum P_T \rangle$ and $\langle \sum P_T^2 \rangle$ are shown in figs. 1, 2, 3 and 4 respectively as a function of c.m. energy. Tables 1 to IV contain a summary of our measured values. For the sake of completeness three sets of values i.e. measured with respect to the thrust and sphericity axis as well as those corrected with respect to the most energetic parton direction are given.

The effects of jet broadening are clearly seen in the data. They are particularly strong in $\langle \sum P_T \rangle$ and $\langle \sum P_T^2 \rangle$. The increase with energy of the values for $\langle P_T \rangle$ and $\langle P_T^2 \rangle$ has been already reported at the level of observed quantities in earlier publications [2]. There it was already stated that these effects are in disagreement with the expectations from the quark-parton model with fragmentation as implemented in the Field-Feynman model. The data are reasonably described if QCD corrections are included following for instance Hoyer et al [7] (solid curves in figs. 1 and 2).

Recently the possibility of describing this jet broadening by perturbative QCD calculations, where the effects of soft gluon corrections are taken into account within the leading log approximation, has been studied [9]. The authors of Ref. [9] find the variables $\langle \sum P_T \rangle$ and $\langle \sum P_T^2 \rangle$ best suited to this purpose and predict

$$\langle \sum P_T \rangle = 1.29 \alpha_s(s) \sqrt{s} \quad (1)$$

and

$$\langle \sum P_T^2 \rangle = 2 \frac{\alpha_s(s)}{3\pi} s \left\{ 0.1365 (M_q(2,s) + M_q^-(2,s)) + 0.2324 M_g(2,s) \right\} \quad (2)$$

with $M_q(n,s)$, $M_q^-(n,s)$ and $M_g(n,s)$ the n th moments of quark, antiquark and gluon fragmentation functions defined as

$$M_a(n,s) = \int dz z^n D_a(z,s) \quad a=q,\bar{q},g \quad (3)$$

where the D_a describes the fragmentation of parton a with energy \sqrt{s} into unspecified hadrons of fractional energy z .

Eq. (1) which is constructed from the first moments of the quark and gluon fragmentation functions, is independent from fragmentation effects due to the trivial relation $M(1,s)=1$. It shows the linear rise of the transverse momenta characteristic of perturbative field theories, damped by the running of the coupling constant. The results of fitting this prediction to our data, referred to the sphericity axis, are also shown in fig 3. The resulting χ^2 is 9 for 8 degrees of freedom and the best estimate for Λ , the only free parameter entering in the fit through the relation $\alpha_s = 4\pi/b \cdot \ln(s/\Lambda^2)$, is 600 ± 25 MeV. This corresponds to $\alpha_s(900 \text{ GeV}^2) = 0.20 \pm 0.01$ in reasonable agreement with previous results derived from the energy dependence of various jet measures [13]. Corresponding fits using the data for the thrust or quark axis yield a value of $\Lambda=667 \pm 20$ MeV thus indicating a systematic error for $\alpha_s(900 \text{ GeV}^2)$ of slightly less than 0.01 from the choice of jet axis.

An estimate of the systematic uncertainty introduced by the fragmentation effects may be obtained by assuming that a detector could reconstruct all primary pseudoscalar and vector mesons from their decay products, and by calculating $\langle \sum P_T \rangle$ from these primary mesons. If this exercise is performed with the help of the Field-Feynman fragmentation model, one obtains values for α_s which are 25% lower than those from the decay products. The ratio of the two results is independent of the c.m. energy, so that it is not possible to resolve it by extrapolating the energy dependence to asymptotia like in other jet observables ($\langle 1-T \rangle$ or $\langle M^2/s \rangle$

, see ref. [13]). It thus appears that the simple prediction (1), in spite of the striking agreement with the energy dependence of $\langle \sum P_T \rangle$, cannot be used for a precise determination of the strong coupling constant.

Inserting plausible assumptions about the quark and gluon fragmentation functions, their scaling violating s-dependence [10,11], and an additive constant (=1) accounting for non-leading corrections to (2), the authors of Ref. [9] predict an energy dependence of $\langle \sum P_T^2 \rangle$ as given by the shaded area in fig. 4. In comparison, the rise of our data appears to be stronger. We have checked that the moment $M(2,s)$ as measured by PLUTO [14] agrees too well with the one assumed in ref. 9 as to explain the discrepancy. We have further verified that the difference cannot be due to the fragmentation effects induced by the decay of vector mesons. In fact the data on $\langle \sum P_T^2 \rangle$ corrected at the level of primary mesons agree in normalization and shape with that corrected at the level of final state hadrons within 15%.

To summarize, mean values $\langle P_T \rangle$, $\langle P_T^2 \rangle$, $\langle \sum P_T \rangle$, and $\langle \sum P_T^2 \rangle$ are presented over a wide energy range. They have been corrected for detector acceptance and resolution as well as for radiative effects in the initial state. Signs of jet broadening are clearly present in the data. This is inconsistent with the expectations from the quark-parton model where the transverse spectra of jets should be energy independent. A good description of the data can be obtained by Monte Carlo calculations where hard gluon emission is taken into account. The energy dependence of the mean total transverse momenta $\langle \sum P_T \rangle$ appears to agree with a QCD calculation, where the broadening is attributed to the effects of gluon radiation as calculated in the LLA. On the other hand, the predicted independence on fragmentation is not observed in the data. The strong coupling constant $\alpha_s(s=900 \text{ GeV}^2)$ comes out to be 0.20 or 0.15, depending on whether the LLA prediction is applied to the data at the final state hadron or the primary meson level. The quantity $\langle \sum P_T^2 \rangle$ shows a dramatic increase with energy. Here the corresponding QCD prediction Eq.(2), which is explicitly dependent on moments of the quark and gluon fragmentation functions, does not properly describe the data. Monte Carlo calculations including complete second order effects [15] describe properly the data thus indicating that $\langle \sum P_T^2 \rangle$ receives non-negligible contributions from fragmentation processes.

ACKNOWLEDGEMENTS : We wish to thank the members of the DESY directorate for the hospitality extended to the university groups. We are grateful to Dr. A. Ali for helpful discussions. We are indebted to the PETRA machine group and the DESY computer center for their excellent performance during the experiment. We gratefully acknowledge the efforts of all engineers and technicians who have participated in the construction and maintenance of the apparatus.

REFERENCES

1. J. Ellis et al., Nucl. Phys. B111 (1976) 253
P. Hoyer et al., see ref. 7 below
2.
 - a) PLUTO Coll., Ch. Berger et al., Phys. Lett. 78B (1978) 176 and 86B (1979) 418
 - b) TASSO Coll., R. Brandelik et al., Phys. Lett. 86B (1979) 243 and 89B (1980) 418
 - c) MARK J Coll., D. P. Barber et al., Phys. Rev. Lett. 43 (1979) 830
 - d) JADE Coll., W. Bartel et al., Phys. Lett. 91B (1980) 142
3. P. C. Bosetti et al., Nucl. Phys. B149 (1979) 13
4. L. Criegee and G. Knies, Phys. Rep. 83 (1982) 153
5.
 - a) S. Brandt et al., Phys. Lett. 12 (1964) 57
 - b) E. Fahri, Phys. Rev. Lett. 39 (1977) 1587
6. R.D. Field and R.P. Feynman, Nucl. Phys. B 136 (1978) 1
7. P. Hoyer et al., Nucl. Phys. B161 (1978) 349
8. J.D. Bjorken and S. Brodsky, Phys. Rev. D1 (1970) 1416
9. P.E.L. Rakow and B.R. Webber, Nucl. Phys. B191 (1981) 63
10. A. H. Mueller, Phys. Rev. D9 (1974) 963
11. C. G. Callan jr. and M. L. Goldberger, Phys. Rev. D11 (1975) 1542
12. J. Babcock and R. E. Cutcosky, Nucl. Phys. B176 (1980) 113
13. PLUTO Collaboration, Ch. Berger et al., Z. Phys. C12 (1982) 297
14. PLUTO Collaboration, unpublished
15. A. Ali et al., Phys. Lett. 93B (1980) 155

TABLE CAPTIONS

- Table I : $\langle P_T \rangle$ values as a function of c.m. energy, measured with respect to the sphericity, thrust and most energetic parton axis.
- Table II : $\langle P_T^2 \rangle$ values as a function of c.m. energy, measured with respect to the sphericity, thrust and most energetic parton axis
- Table III : $\langle \sum P_T \rangle$ values as a function of c.m. energy, measured with respect to the sphericity, thrust and most energetic parton axis.
- Table IV : $\langle \sum P_T^2 \rangle$ values as a function of c.m. energy, measured with respect to the sphericity, thrust and most energetic parton axis.

FIGURE CAPTIONS

- 1) $\langle P_T \rangle$ as a function of c.m. energy. The full (open) circles refer to $\langle P_T \rangle$ values obtained with respect to the thrust (sphericity) axis. The open triangles refer to values obtained with respect to the most energetic parton direction. The solid curve represents the expectations from the Field-Feynman Monte Carlo for energies below 17 GeV, and those from Hoyer et al. for energies above. Note the bb threshold near $\sqrt{s} = 10$ GeV in this and the following figures.
- 2) $\langle P_T^2 \rangle$ as a function of c.m. energy. The full (open) circles refer to $\langle P_T^2 \rangle$ values obtained with respect to the thrust (sphericity) axis. The open triangles refer to values obtained with respect to the most energetic parton direction. For comparison data from the TASSO Collaboration [2b] are also shown, full triangles. The solid curve represents expectations from Monte Carlo models as in fig. 1.
- 3) $\langle \sum P_T \rangle / s$ as function of c.m. energy. The full points refer to $\langle \sum P_T \rangle$ values obtained with respect to the thrust (sphericity) axis. The open triangles refer to values obtained with respect to the most energetic parton direction. The solid line indicates the QCD prediction in LLA of ref. [9] for $\Lambda = 600$ MeV.
- 4) $\langle \sum P_T^2 \rangle$ as a function of c.m. energy. The full (open) circles refer to $\langle \sum P_T^2 \rangle$ values obtained with respect to the thrust (sphericity) axis. The open triangles refer to values obtained with respect to the most energetic parton direction. The evaluation of Eq.(2) according to ref.9 is represented by the shaded area. The solid curve represents the expectations from Ali Monte Carlo [15] including complete second order effects using a value of Λ of 200 MeV. The sphericity axis was considered as jet axis. Similar results are obtained with Hoyer et al. [7].

Energy	$\langle \sum P_T \rangle$ Sphericity axis	$\langle \sum P_T \rangle$ Thrust axis	$\langle \sum P_T \rangle$ Parton axis
7.7	2.93 ± 0.07	3.06 ± 0.06	3.18 ± 0.07
9.4	3.50 ± 0.08	3.61 ± 0.09	3.75 ± 0.10
12.0	4.48 ± 0.13	4.62 ± 0.14	4.71 ± 0.16
13.0	4.39 ± 0.16	4.55 ± 0.16	4.64 ± 0.20
17.0	5.05 ± 0.23	5.15 ± 0.23	5.12 ± 0.22
22.0	6.02 ± 0.48	6.15 ± 0.48	6.11 ± 0.46
27.6	7.31 ± 0.26	7.49 ± 0.26	7.47 ± 0.26
30.0-31.6	8.03 ± 0.23	8.24 ± 0.23	8.22 ± 0.23

Table 3. $\langle \sum P_T \rangle$ (in GeV) as a function of energy

Energy	$\langle \sum P_T^2 \rangle$ Sphericity axis	$\langle \sum P_T^2 \rangle$ Thrust axis	$\langle \sum P_T^2 \rangle$ Parton axis
7.7	1.12 ± 0.03	1.22 ± 0.04	1.34 ± 0.05
9.4	1.54 ± 0.07	1.75 ± 0.08	1.92 ± 0.09
12.0	2.27 ± 0.13	2.48 ± 0.14	2.72 ± 0.16
13.0	2.12 ± 0.14	2.29 ± 0.15	2.51 ± 0.16
17.0	2.53 ± 0.25	2.79 ± 0.28	2.98 ± 0.31
22.0	3.56 ± 0.88	3.70 ± 0.88	3.95 ± 0.94
27.6	4.45 ± 0.40	4.79 ± 0.42	5.17 ± 0.45
30.0-31.6	5.62 ± 0.35	6.29 ± 0.41	6.79 ± 0.45

Table 4. $\langle \sum P_T^2 \rangle$ (in GeV²) as a function of energy

Energy	$\langle P_T \rangle$ Sphericity axis	$\langle P_T \rangle$ Thrust axis	$\langle P_T \rangle$ Parton axis
7.7	285.3 ± 3.3	297.0 ± 3.3	300.1 ± 3.2
9.4	301.1 ± 3.6	313.1 ± 3.7	315.3 ± 3.9
12.0	330.6 ± 6.3	342.7 ± 6.9	350.1 ± 7.2
13.0	329.0 ± 7.9	341.7 ± 8.6	349.1 ± 8.9
17.0	333.9 ± 8.6	339.3 ± 9.7	338.8 ± 9.7
22.0	350.6 ± 18.5	360.9 ± 18.8	358.5 ± 18.7
27.6	369.1 ± 7.9	375.5 ± 9.0	378.1 ± 9.0
30.0-31.6	399.7 ± 6.1	408.6 ± 7.6	411.5 ± 7.6

Table 1. Mean transverse momenta (in MeV) as a function of energy

Energy	$\langle P_T^2 \rangle$ Sphericity axis	$\langle P_T^2 \rangle$ Thrust axis	$\langle P_T^2 \rangle$ Parton axis
7.7	120.0 ± 2.8	131.4 ± 3.3	137.3 ± 4.5
9.4	135.1 ± 3.7	147.3 ± 4.8	154.4 ± 5.0
12.0	168.3 ± 7.4	184.0 ± 8.6	196.3 ± 9.4
13.0	157.9 ± 8.4	171.7 ± 9.6	183.3 ± 10.4
17.0	167.7 ± 11.6	184.2 ± 16.0	184.2 ± 16.0
22.0	207.3 ± 33.1	217.0 ± 35.8	214.8 ± 35.4
27.6	224.7 ± 14.9	239.2 ± 18.6	245.6 ± 18.6
30.0-31.6	279.8 ± 12.7	311.4 ± 17.8	319.7 ± 17.4

Table 2. Mean transverse momenta squared (in MeV²) as a function of energy

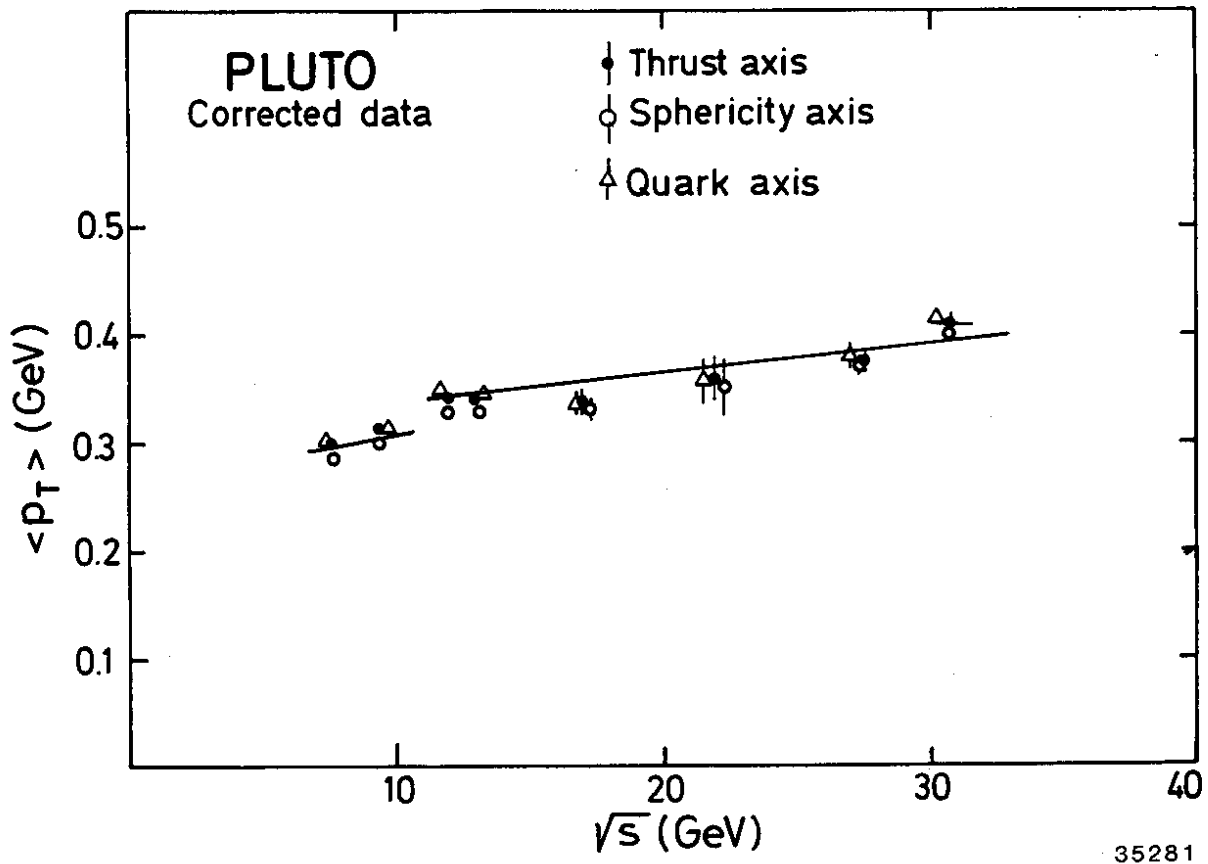


Fig. 1

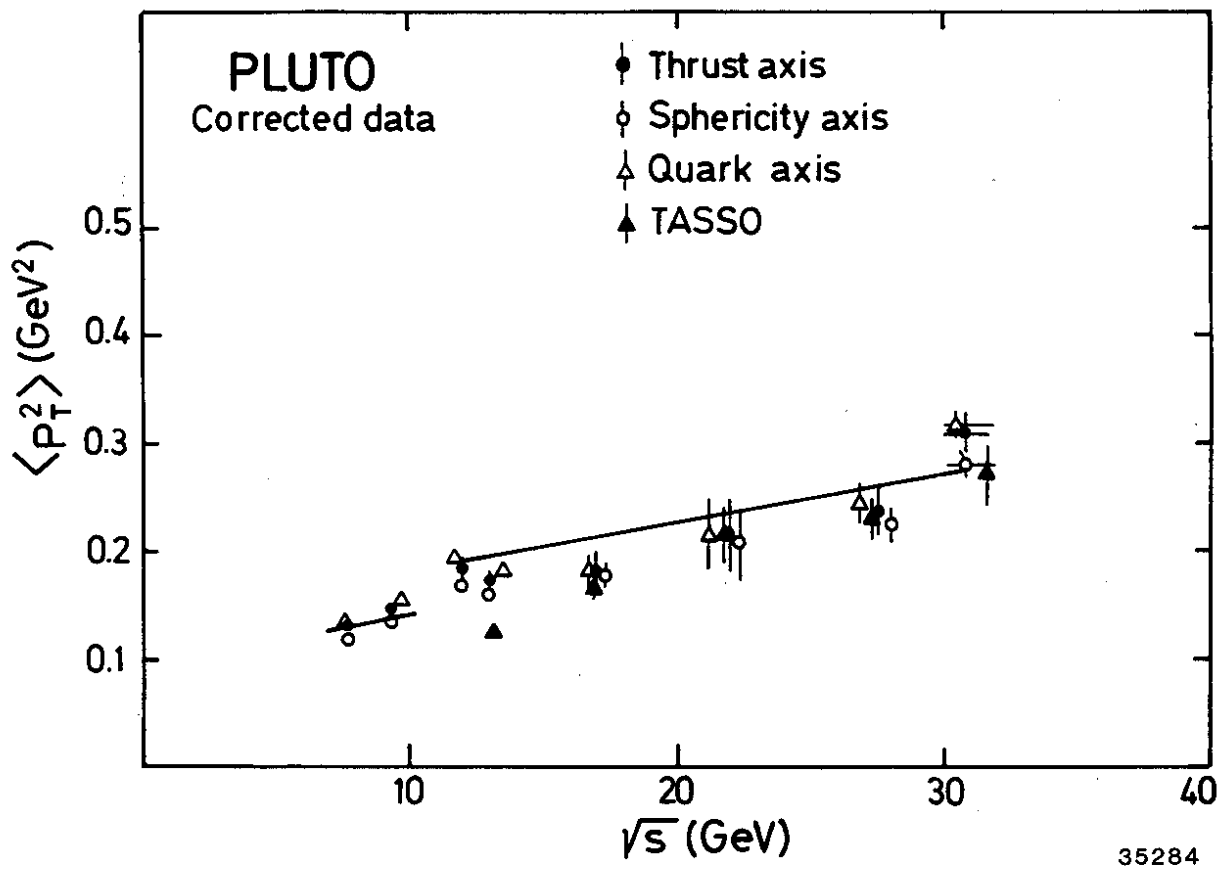


Fig. 2

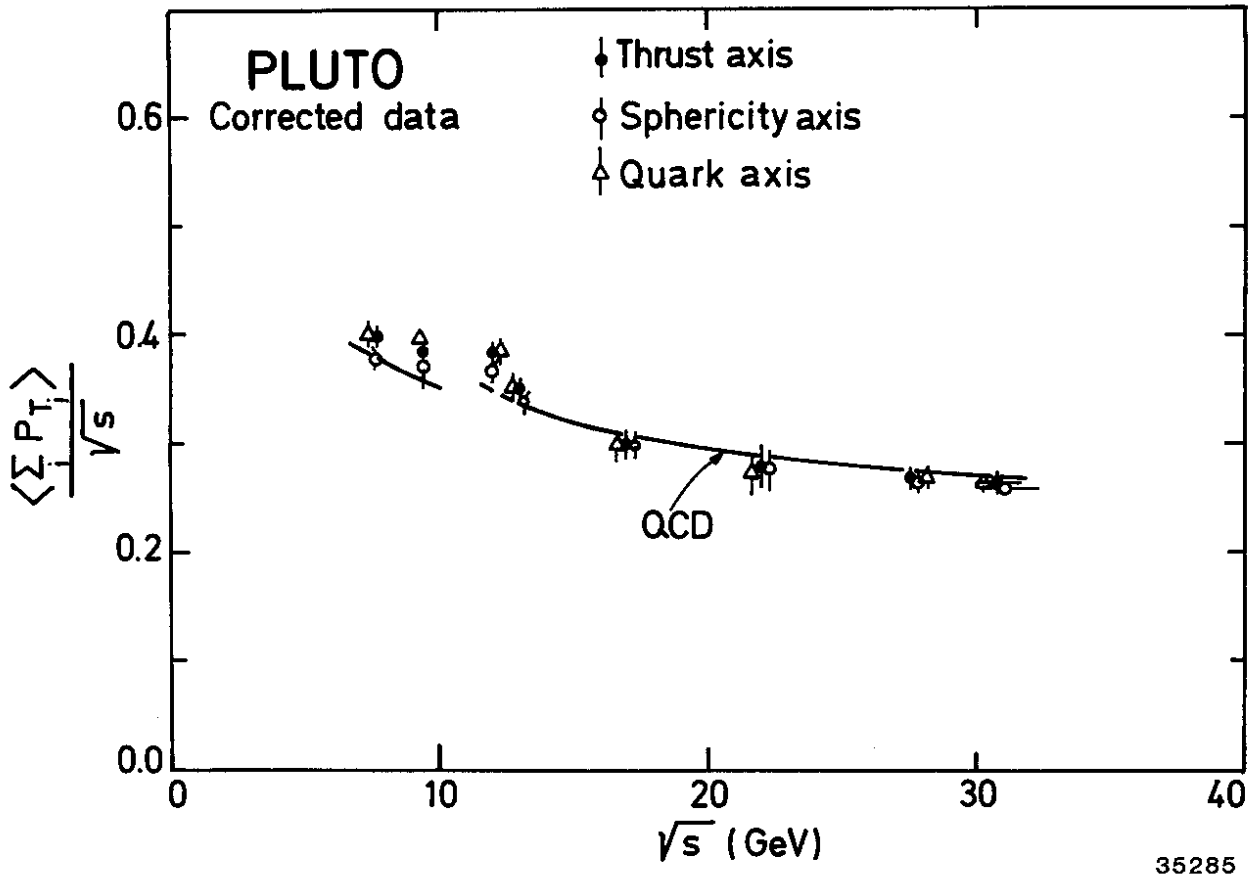


Fig. 3

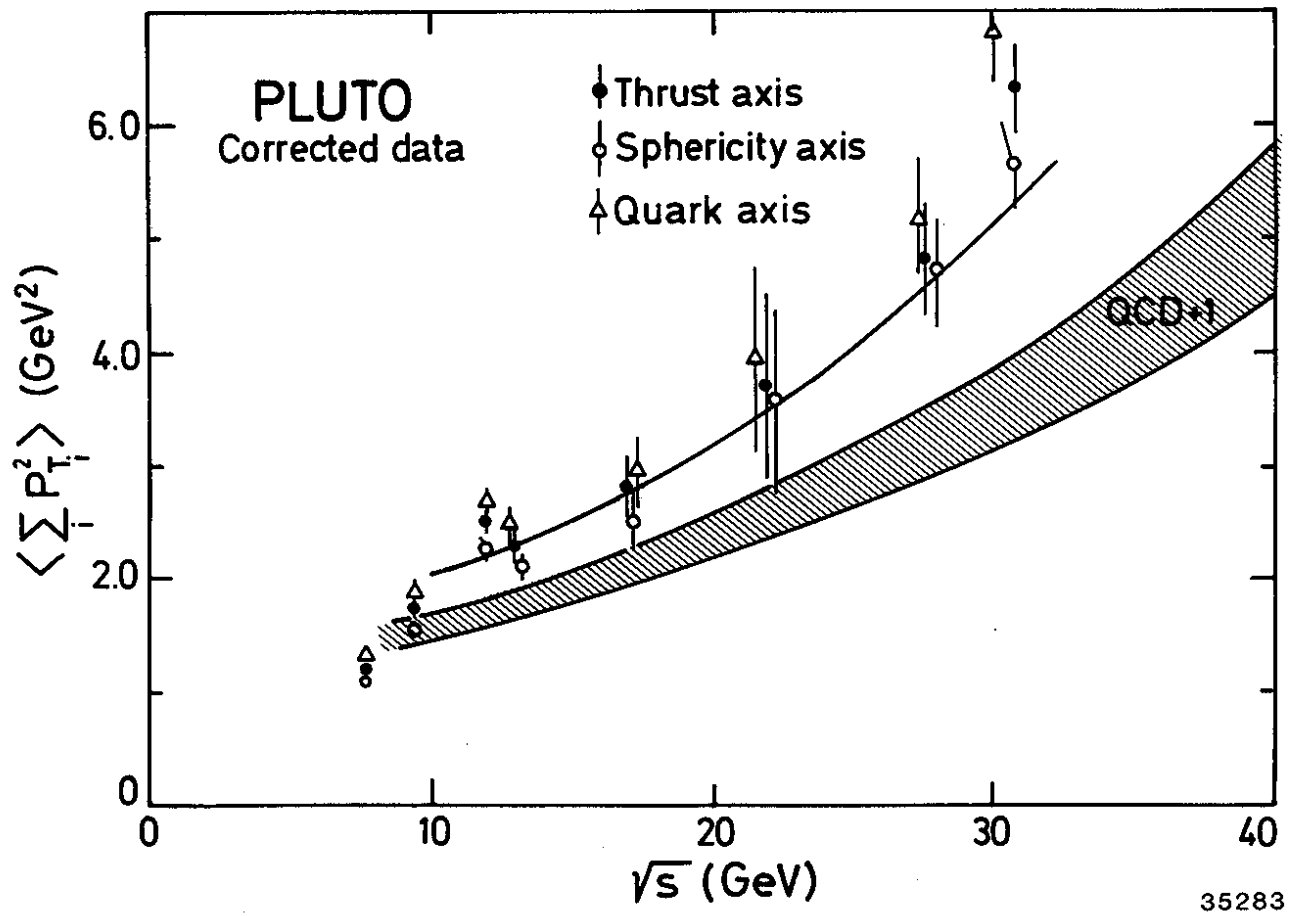


Fig. 4